American Journal of Electromagnetics and Applications
2017; 5(2): 14-19
http://www.sciencepublishinggroup.com/j/ajea
doi: 10.11648/j.ajea.20170502.11
ISSN: 2376-5968 (Print); ISSN: 2376-5984 (Online)

Review Article

FDTD Simulations of Surface Plasmons Using the Effective Permittivity Applied to the Dispersive Media

Otman Sofiane, Said Ouaskit

Physics Department, Faculty of Science Ben M'Sik, Hassan II University, Casablanca, Morocco

Email address:
sofiane.otman@gmail.com (O. Sofiane), s.ouaskit@gmail.com (S. Ouaskit)

To cite this article:
Otman Sofiane, Said Ouaskit. FDTD Simulations of Surface Plasmons Using the Effective Permittivity Applied to the Dispersive Media. *American Journal of Electromagnetics and Applications.* Vol. 5, No. 2, 2017, pp. 14-19. doi: 10.11648/j.ajea.20170502.11

Received: August 11, 2017; **Accepted**: August 29, 2017; **Published**: October 11, 2017

Abstract: This paper presents the analysis of electromagnetic fields in random metallic materials for plasmonics applications. In this context, the two-dimensional finite- difference time-domain (2D-FDTD) method is used to simulate the surface Plasmons (SPs), with the perfectly matched layer (PML). To solve the problem, the idea of effective permittivity for the curved surface is applied to the dispersive media, while the Z-transform method is applied to the Drude model. The numerical results obtained by 2D -FDTD for circular silver cylinders are given and discussed.

Keywords: FDTD, Surface Plasmon, Effective Permittivity, Dispersive Media, Z-Transform

1. Introduction

In recent years, SPs have been applied to advanced optical devices, such as sensors, microscopies, lasers, and hyperlenses. A SP may be defined classically as "a fundamental electromagnetic mode of an interface between a material with a negative permittivity and a material with a positive permittivity having a well-defined frequency and which involves electronic surface-charge oscillation" [1].

The first scientific observations of SP were reported at the beginning of the twentieth century [2], when Wood, in 1902, observed an anomalous intensity drops in spectra produced when visible light reflects at metallic gratings [4].More than 30 years later, Fano established another explanation of Wood's anomalies[5]. Around this time, Ritchie reported the abnormal behavior of metal gratings in terms of excited surface plasmon resonance modes [6].In the same year, Otto [7], Kretschmann and Raether [8] presented methods to optically excited surface plasmon on metal surfaces. Since this pioneer study, various metallic nanostructures are reported for nano-plasmonic devices [3, 9, 10, 12, 13, 14].

Numerical simulations are useful to analyze the complicated structures of these devices. In this context, the FDTD method [18, 19, 21, 22] is seen as the most popular numerical technique in the simulation of plasmonic structure.

Since 1966, the FDTD method has been successfully applied by Yee [17], to various electromagnetic problems and phenomena, such as plasmonic applications [16]. Then the FDTD method can model propagation in dispersive media known as Drude material [16], [19]. The z-transform approach was applied to describe the complex permittivity and its frequency dependence of the medium [20]. The effective Permittivity at the curved material interfaces [24, 25, 26] was used to take into count the geometry of the system with the PML absorbing boundary conditions [23].

In this paper, the numerical 2D-FDTD simulation results are showed for silver cylinders immersed in a dielectric medium.

2. FDTD Method

Following the study for a SP, the FDTD method was applied to simulate light interaction by particles of cylindrical shapes immersed in dielectric medium. The first start is from Maxwell's equations. These can be expressed in differential form as:

$$\nabla \times E = -\frac{\partial B}{\partial t} \tag{1}$$

$$\nabla \times H = \frac{\partial D}{\partial t} \tag{2}$$

Where B is the magnetic flux density, D is the electric flux density, E is the electric field intensity and H is the magnetic field intensity.

In the following, the media are assumed that $J = 0$ and $\rho = 0$, that is to say there is no flow of current and no free charges. Assume also nonmagnetic material and therefore set $\mu = \mu 0$.

The flux densities and the field intensities are related through the constitutive relations. For linear, isotropic media, these are:

$$D = \varepsilon E \tag{3}$$

$$B = \mu H \tag{4}$$

where ε and μ are respectively the permittivity and the permeability of the media.

Substituting the space and time derivatives by central differences using a staggered mesh, where the electric and magnetic fields components are located at different points. For the time derivative, the electric and magnetic fields are disposed according to the leapfrog scheme.

So the time and space evolutions of every field component which casted in the form suitable for 2D discretization in space and time domain [18, 21] can be written as, for example the z component of the electric field:

$$\frac{E_z^{n+1}(i,j) - E_z^n(i,j)}{\Delta t} = \frac{1}{\varepsilon}\left(\frac{H_y^{n+\frac{1}{2}}(i+\frac{1}{2},j) - H_y^{n+\frac{1}{2}}(i-\frac{1}{2},j)}{\Delta x} - \frac{H_x^{n+\frac{1}{2}}(i,j+\frac{1}{2}) - H_x^{n+\frac{1}{2}}(i,j-\frac{1}{2})}{\Delta y}\right) \tag{5}$$

where n, i, j are integers that are running on the space and time mesh, Δx and Δyare the space mesh steps and Δt is the time mesh step.

Checking the Courant–Friedrich–Levy stability condition [18], if the time-step is larger than the Courant limit, the method becomes unstable, thus the time-step must be very small.

The PML [23] was applied as an absorbing boundary condition to truncate the computational grids.

3. Effective Permittivity for Plasmonic Materials

At nano scale, the nano structured materials present many interesting optical properties; the Plasmonic technologies exploit the optical electromagnetic wave propagation locally confined to a metal-dielectric interface [15].

The optical properties of a medium and its interaction with an external excitation electromagnetic wave is described by the dielectric response function $\varepsilon_1(\omega)$. In this work the well known single-pole Drude dispersion form of $\varepsilon_1(\omega)$ is used to describe the silver cylinder-dielectric response[18]:

$$\varepsilon_1(\omega) = 1 - \frac{\omega_p^2}{\omega^2 + i\nu_c\omega} \tag{6}$$

Where ω_p is the plasma frequency and ν_c is the collision frequency. The dielectric medium is characterized by the real permittivity ε_2 which depends slightly on the excitation wave frequency**.**

The staircased effective permittivity (S-EP) model for FDTD computation of plasmonic materials is based to represent curved plasmonic surfaces in 2-D Cartesian-cell FDTD grids [27]. The S-EP method is implemented only by changing permittivity values assigned to Ecomponents near the surface of a plasmonic medium.

The Effective Permittivity in a general form is given by [24, 25, 26]:

$$\varepsilon_{eff} = \varepsilon_{\parallel}(1 - n^2) + \varepsilon_{\perp} n^2 \tag{7}$$

Where n is the projection of the unit normal vector n along the field, $\varepsilon_{\parallel}$ and $\varepsilon_{\perp}$ are parallel and perpendicular permittivity to the material interface, respectively and defined as:

$$\varepsilon_{\parallel} = f\varepsilon_2 + (1-f)\varepsilon_1 \tag{8}$$

$$\varepsilon_{\perp} = \left[\frac{f}{\varepsilon_2} + \frac{(1-f)}{\varepsilon_1}\right]^{-1} \tag{9}$$

where f is the filling ratio of metal in a certain FDTD cell.

Finally, the Z-transform technique [20] was used to calculate the electric field from the electric flux density:

$$D(\omega) = \varepsilon_0 \varepsilon_1(\omega) E(\omega) \tag{10}$$

where ε_o is the free-space permittivity.

4. Numerical Results

In this simulation, a monochromatic Gaussian plane wave source with TMz polarized waves illuminates metallic cylinder with radius r=15 nm and permittivity ε_2, immersed in dielectric medium (air) has the permittivity ε_2 as shown in Figure 1.

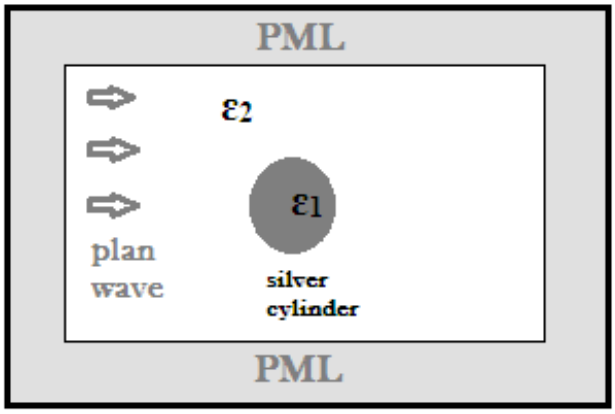

Figure 1. *Computational Setup: an Incident TMz polarization illuminate silver cylinder with permittivity ε_1 immersed in the dielectric medium with permittivity ε_2.*

The operating frequency of the incident plane wave is f=750 THz, which corresponds to the wavelength in free space, λ=400nm.

The 2D- FDTD computational domain is discretized with 200 ∗ 200 Yee cells, and is terminated in 10-cell. PMLs were used to truncate the simulation region with the condition [23]:

$$\frac{\sigma}{\varepsilon_0} = \frac{\sigma^*}{\mu_0} \tag{11}$$

Where ε_0 and μ_0 are the permittivity and permeability of free space, σ is the specific conductivity, σ * is a nonphysical parameter that allows the absorption of the magnetic field to be symmetrized with respect to the absorption of the electric field.

The spatial discretization is uniform, and can be given as $\Delta x = \Delta y = 10^{-9}$ m. The time step is chosen to satisfy the Courant–Friedich–Levy (CFL) condition for FDTD algorithm as:

$$dt = \frac{dx}{\sqrt{2}c} \tag{12}$$

where c is the speed of light in the free space.

In each of these examples, the silver cylinder was assumed to be characterized by the following Drude model parameters in [15, 19]: ε_∞ = 1; $\omega_p = 1.256 .10^{16}$ rad/s;

$$\nu c = 5.7 . 10^{13} \text{ s}^{-1}$$

The dielectric medium (air) has been characterized by the permittivity ε_2=1.

The incident, total and scattered electric field distribution respectively $E_{z\,inc}$, $E_{z\,tot}$ and $E_{z\,scat}$, and also the two components of magnetic field respectively H_x and H_y in the near field is simulated using the 2D-FDTD method as shown in Figure 2; Figure 3; Figure 4 and Figure 5 respectively.

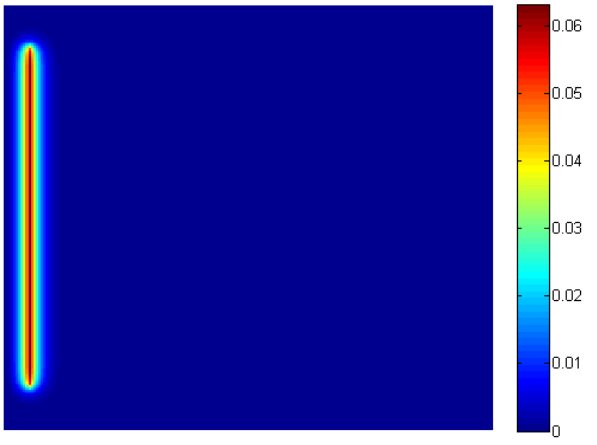

Figure 2. *Visualization of the FDTD-computed Ez incident wave along the x-y planar before the traveling time between the source and silver cylinder surface.*

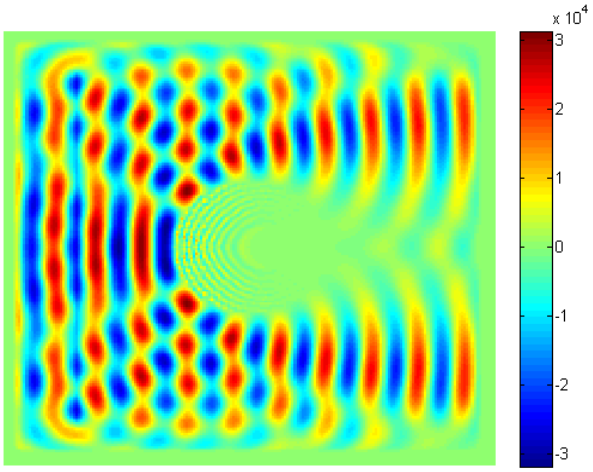

Figure 3. *Visualization of the FDTD-computed Ez total field distribution along the x-y planar.*

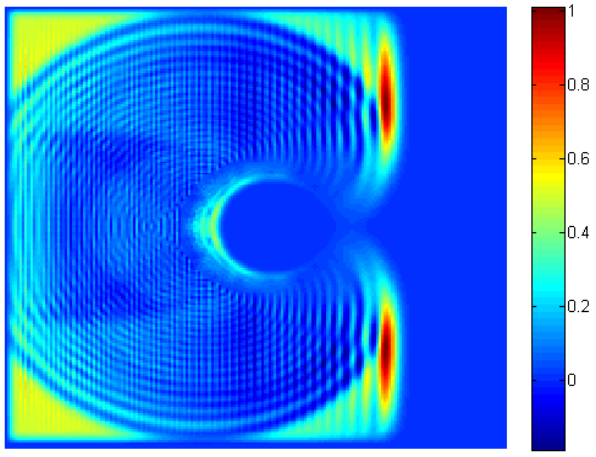

Figure 4. *Visualization of the FDTD-computed E_z scattered field distribution along the x-y planar.*

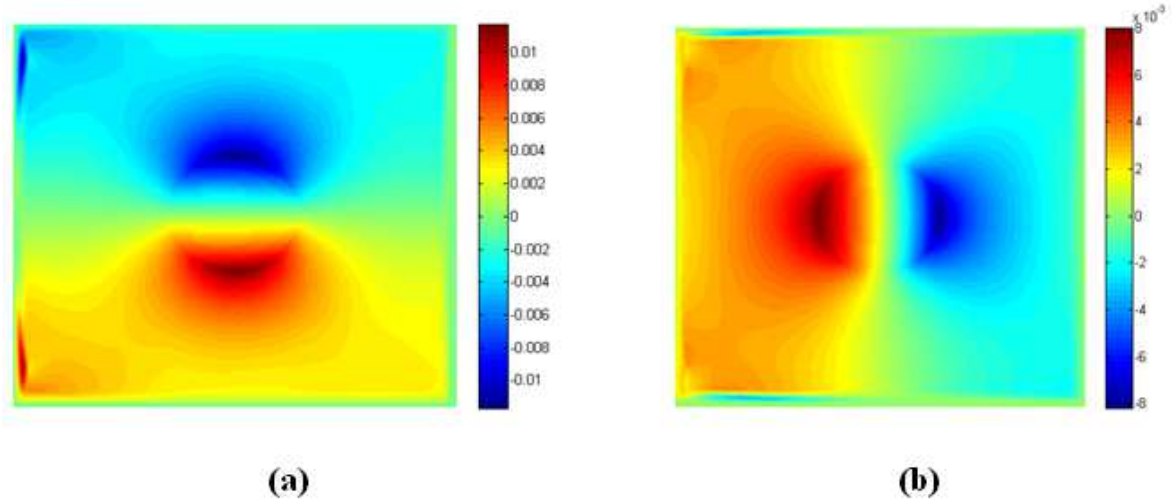

Figure 5. *Visualization of the FDTD-computed magnetic field distribution along the x-y planar: (a) H_x component; (b) H_y component.*

From the two dimensional field distribution which arrive one dimensional spatial field distribution along x axis. The Figure 6(a) and Figure 6(b) showed respectively the amplitude and intensity of the electric field along the x axis with (y=100, z=0) corresponding to the cylinder center coordinate.

Figure 6(a) shows an enhancement of field amplitude implying that an oscillating surface charge has been involved by the incident plane wave. This is the localized SP.

In Figure 6(a), oscillations of several periods and different amplitudes can be observed; they are due to the interference between the excited and scattered waves. The oscillations of short period and small amplitude in the region x<70 and x>130 are due to the interference between the incidence and the scattered waves. The peak of the electric field amplitude at the surface is greater than that of the incident field amplitude by nearly an order of magnitude. The electric field inside the cylinder made negligible.

A plot of the square of electric field in Figure 6(b) shows that the field intensity is much stronger at the surface of cylinder.

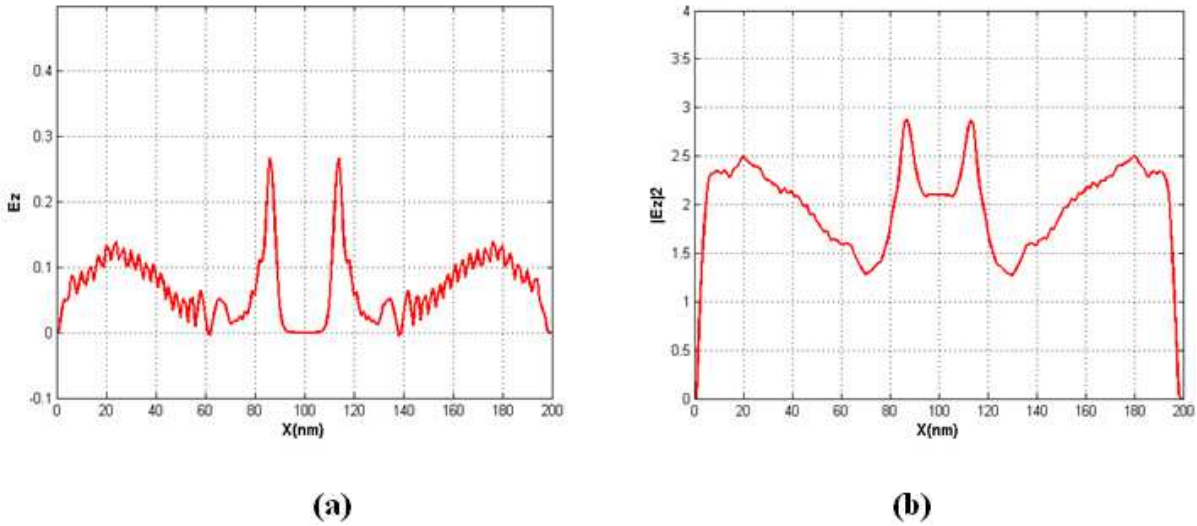

Figure 6. *The spatial configurations of the Electric field enhancement along x axis: (a) the evolution of the electric field at the center(y=100); (b)his intensity (maxima normalized).*

The magnetic field H_x amplitude and intensity are respectively plotted, in Figure 7(a) and Figure 7(b), as function of x along the axis in the two dielectric-metal interfaces (at y=85 and y=115) for z=0. The maximum of the intensity is approximately two times higher than the incidence.

The magnetic field H_y amplitude and intensity are respectively plotted, in Figure 8(a) and Figure 8(b), as function of x along the axis in the dielectric-metal interface and the centre of cylinder (at y=85 and y=100) for z=0. It may be seen that H_y is continuous and changes sign at the two dielectric-metal interfaces.

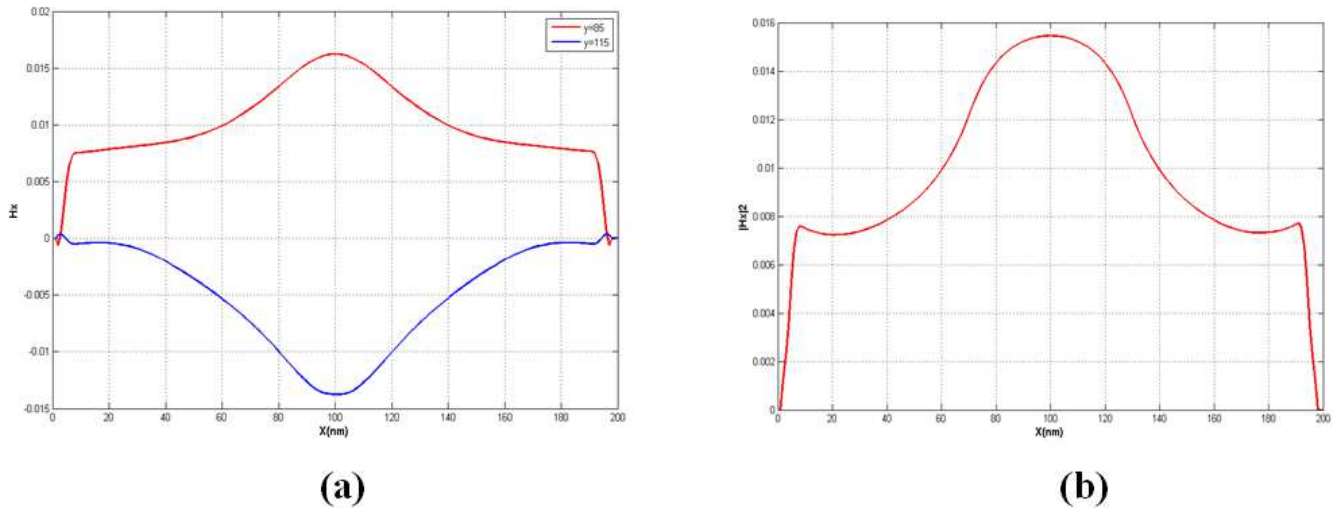

Figure 7. *The spatial configurations of the H_x component of the magnetic field enhancement along x axis.(a) the evolution of H_x component in the two dielectric-metal interfaces (at y=85 and y=115); (b) their intensity (maxima normalized).*

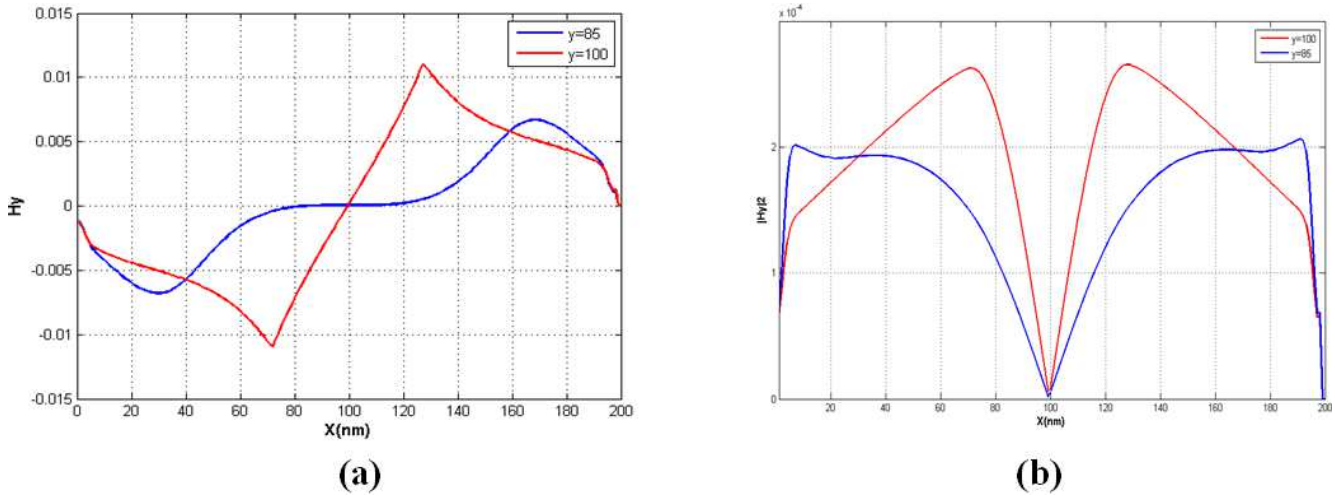

Figure 8. *The spatial configurations of the H_y component of the magnetic field enhancement along x axis: (a) the evolution of H_y component at the center(y=100) and the interface (y=85); (b) the distribution of their intensities.*

5. Conclusions

This work proposed a S-EP model based FDTD computation of plasmonic materials.

FDTD simulations using the S-EP model were implemented for the infinitely-long Ag cylinder. A monochromatic Gaussian plane wave source illuminate the metallic cylinder with the complex permittivity ε(ω) immersed in dielectric medium, the method is based on Drude dispersive model which is incorporated into Maxwell equations. Z-transform technique was used to analyze the stability and the accuracy of finite-difference time-domain (FDTD) algorithms and the PML was usedto truncate the computational grids.

In this study the distribution of electromagnetic fields in the x-y planar has been described and simulated, and the spatial configurations of the near-fields enhancement along x axis and their intensities are plotted where clearly verified the applicability of the FDTD to model the metallic nanoparticle.

The proposed model and simulation can be applied to other dispersion medium, because it is implemented only by changing how permittivity values are assigned to grid points.

References

[1] Sarid, D.; Challener, W. Modern Introduction to Surface Plasmons theory mathematica modeling and applications; Cambridge University Press, 2010.

[2] Rivera, V. A. G.; Silva, O. B.; Ledemi, Y.; Messaddeq, Y.; Marega, E. Collective Plasmon-Modes in Gain Media Quantum Emitters and Plasmonic Nanostructures; Springer, 2015.

[3] Homola, J. Surface Plasmon Resonance Based Sensors; Springer, 2006; 04.

[4] Wood, R. W. On a remarkable case of uneven distribution of light in a diffraction grating spectrum; Phil, Mag, 1902; 4, 396.

[5] Fano, U. Atomic Theory of electromagnetic interactions in dense materials; Physical Review 1956. 103, 1202.

[6] R. H. Ritchie, E. T. Arakawa, J. J. Cowan, and R. N. Hamm. Surface-plasmon resonance effect in grating diffraction; Physical Review letters 1968. 21, 1530-1532.

[7] Otto, A. Excitation of nonradiative surface plasma waves in silver by the method of frustrated total reflection; Z. Phys 1968. 216, 398.

[8] Kretschmann, E.; Raether, H. Radiative decay of nonradiative surface plasmons excited by light; Z. Naturforsch 1968. 23A, 2135.

[9] W. A. Challener, I. K. Sendur; C. Peng. Scattered field formulation of finite difference time domain for a focused light beam in dense media with lossy materials; optics express 2003. Vol. 11, No. 23, 3160-3170.

[10] Chris D. Geddes. Reviews in plasmonics 2015; Springer International Publishing Switzerland 2016.

[11] Chris D. Geddes. Surface Plasmon Enhanced, Coupled and Controlled Fluorescence; John Wiley & Sons, Inc 2017.

[12] Mark, L. Brongersma; Pieter, G. Kik. Surface Plasmon Nanophotonics; Springer, 2007.

[13] Tigran, V. Shahbazyan; Mark, I. Stockman. Plasmonics Theory and Applications; Springer, 2013.

[14] Stefan, A. Maier. Plasmonics Fundamentals and Applications; Springer, 2007.

[15] Nico, J. de Mol; Marcel, J. E. Fischer. Surface Plasmon Resonance Methods and Protocol; Humana Press, 2010.

[16] Ahmed, I.; E. H. Khoo; O. Kurniawan; E. P. Li. Modeling and simulation of active plasmonics with the FDTD method by using solid state and Lorentz–Drude dispersive model. Optical Society of America B, Vol. 28, 2011, pp. 352–359.

[17] Yee, K. S. Numerical Solution of Initial Boundary Value Problems Involving Maxwell's Equations in Isotropic Media; IEEE Trans. Antennas Propagat. 1966, AP-14, 302–307.

[18] Taflove, A.; Hagness, S. C. Computational Electrodynamics The Finite-Difference Time-Domain Method, 3rd ed.; Artech House, 2005.

[19] Kunz, K. S.; Luebbers, R. J. The Finite Difference Time Domain Method for Electromagnetics; CRC Press, Boca Raton, 1993.

[20] Sullivan, D. M. Electromagnetic Simulation Using the FDTD Method; New York, IEEE Press, 2000.

[21] Umran, S. Inan; Robert A. Marshall. Numerical Electromagnetics The FDTD Method; Cambridge University Press, 2011.

[22] Ramesh Garg. Analytical and Computational Methods in Electromagnetics; Artech House, 2008.

[23] Berenger, J. R. A perfectly matched layer for the absorption of electromagnetic waves; J. Computat. Phys. 1994, 114, 185-200.

[24] Zhao, Y.; Hao, Y. Finite-difference time-domain study of guided modes in nano-plasmonic waveguides; IEEE Trans. Antennas Propag. 2007, 55, 3070–3077.

[25] Zhao, Y.; Hao, Y. Conformal Dispersive Finite-Difference Time-Domain Simulations of Plasmonic Waveguides; IEICE 2007, 224-227.

[26] Mohammadi, A.; Jalali, T.; Agio, M. Dispersive contour-path algorithm for the two-dimensional finite difference time-domain method; Optics Express 2008, 16, 7397-7406.

[27] Okada, N.; Cole, J. B. Effective permittivity for FDTD calculation of plasmonic materials; Micromachines 2012, 3, 168–179.